Clinical Biomechanics 28 (2013) 378–385

Contents lists available at SciVerse ScienceDirect

Clinical Biomechanics

journal homepage: www.elsevier.com/locate/clinbiomech

A theoretical analysis of the influence of wheelchair seat position on upper extremity demand

Jonathan S. Slowik, Richard R. Neptune *

Department of Mechanical Engineering, The University of Texas at Austin, Austin, TX, USA

ARTICLE INFO

Article history:
Received 10 October 2012
Accepted 13 March 2013

Keywords:
Forward dynamics simulation
Musculoskeletal model
Biomechanics
Wheelchair propulsion
Muscle stress
Co-contraction
Metabolic cost

ABSTRACT

Background: The high physical demands placed on the upper extremity during manual wheelchair propulsion can lead to pain and overuse injuries that further reduce user independence and quality of life. Seat position is an adjustable parameter that can influence the mechanical loads placed on the upper extremity. The purpose of this study was to use a musculoskeletal model and forward dynamics simulations of wheelchair propulsion to identify the optimal seat position that minimizes various measures of upper extremity demand including muscle stress, co-contraction and metabolic cost.
Methods: Forward dynamics simulations of wheelchair propulsion were generated across a range of feasible seat positions by minimizing the change in handrim forces and muscle-produced joint moments. Resulting muscle stress, co-contraction and metabolic cost were examined to determine the optimal seat position that minimized these values.
Findings: Muscle stress and metabolic cost were near minimal values at superior/inferior positions corresponding to top-dead-center elbow angles between 110 and 120° while at an anterior/posterior position with a hub-shoulder angle between −10 and −2.5°. This coincided with a reduction in the level of muscle co-contraction, primarily at the glenohumeral joint.
Interpretation: Deviations from this position lead to increased co-contraction to maintain a stable, smooth propulsive stroke, which consequentially increases upper extremity demand. These results agree with previous clinical guidelines for positioning the seat to reduce upper extremity overuse injuries and pain for wheelchair users.
© 2013 Elsevier Ltd. All rights reserved.

1. Introduction

There are approximately 3.3 million wheelchair users in the United States (CDC, 2009), with the vast majority (>90%) of users relying on manual wheelchair propulsion as their primary method of mobility (Kaye et al., 2000). Upper extremity pain and injuries that frequently occur in wheelchair users can be extremely debilitating and lead to a decrease in independence and quality of life (e.g., Gutierrez et al., 2007). The high incidence of pain and injury is correlated with the high physical demand placed on the upper extremity during wheelchair propulsion (e.g., Curtis et al., 1999). In addition to generating the mechanical power required to propel the wheelchair, the upper extremity muscles must also help maintain joint stability (e.g., Requejo et al., 2008). These stability requirements, along with the kinematic constraints of the push phase, require significant intermuscular coordination and co-contraction (e.g., Rankin et al., 2010, 2011, 2012; van der Helm and Veeger, 1996). Although co-contraction has many beneficial purposes (e.g., helping to stabilize a joint), it can also have detrimental effects (e.g., elevated joint loading and muscle fatigue). Notably, the glenohumeral joint has relatively few stabilizing structures (Veeger and van der Helm, 2007), requiring the muscles responsible for stabilizing the joint to be highly active and have an elevated risk of injury (e.g., Mulroy et al., 2004; Veeger et al., 2002).

Seat position is an easily adjustable parameter that directly influences propulsion mechanics (e.g., Boninger et al., 2000; Gorce and Louis, 2012; Kotajarvi et al., 2004; Richter, 2001) and upper extremity demand (e.g., Gutierrez et al., 2005; Mulroy et al., 2005; Paralyzed Veterans of America Consortium for Spinal Cord Medicine (PVACSCM), 2005; Requejo et al., 2008). Thus, identifying the optimal seat position that minimizes upper extremity demand holds great promise for reducing the risk of pain and injury. A number of studies have examined the influence of seat position on propulsion mechanics and found relationships with specific biomechanical measures such as cadence (e.g., Boninger et al., 2000; Gorce and Louis, 2012; Kotajarvi et al., 2004; Masse et al., 1992; Richter, 2001), handrim forces (e.g., Boninger et al., 2000; Kotajarvi et al., 2004; van der Woude et al., 2009), joint ranges of motion (e.g., Gorce and Louis, 2012; Wei et al., 2003) and electromyography (EMG) activity (e.g., Gutierrez et al., 2005; Louis and Gorce, 2010; Masse et al., 1992). High levels of these measures have been identified as risk factors for upper extremity pain and injury (e.g., Gorce and Louis, 2012; Gutierrez et al., 2005; PVACSCM, 2005).

* Corresponding author at: Department of Mechanical Engineering, The University of Texas at Austin, 204 E. Dean Keeton Street, Stop C2200, Austin, TX 78712, USA.
E-mail address: rneptune@mail.utexas.edu (R.R. Neptune).

0268-0033/$ – see front matter © 2013 Elsevier Ltd. All rights reserved.
http://dx.doi.org/10.1016/j.clinbiomech.2013.03.004

Recent clinical guidelines based on these relationships suggest that seat position should be adjusted as far posterior as possible without compromising wheelchair stability (PVACSCM, 2005). The guidelines also recommend superior/inferior positions that correspond to an elbow angle between 100° and 120° when the hand is at the top-dead-center (TDC) position on the handrim (full extension is 180°). However, recent studies have found with such low, posterior seat positions, the joint ranges of motion and muscle activity levels may be increased (Gorce and Louis, 2012; Louis and Gorce, 2010), which may adversely affect upper extremity demand.

One challenge in assessing the influence of seat position on upper extremity demand is the difficulty in directly measuring demand-related quantities such as muscle stress or co-contraction that may elevate joint loading. Because these measures are difficult to obtain experimentally, indirect measures are frequently used (e.g., Erdemir et al., 2007). For example, inverse dynamics techniques are often used to determine joint moments, but identifying individual muscle force and stress values is challenging due to muscle redundancy and co-contraction (Erdemir et al., 2007; Zajac et al., 2002). In addition, systematically investigating the influence of seat position on upper extremity demand using experimental techniques is difficult and time-consuming (e.g., to assess the influence of seat position on metabolic cost). As a result, most studies have investigated a limited number of seat positions (e.g., two or three).

Forward dynamics simulations provide an alternative approach to systematically examine the influence of wheelchair seat position on direct measures of upper extremity demand. Forward dynamics techniques have been successfully used to analyze various human movement tasks such as pedaling (e.g., Raasch et al., 1997; Rankin and Neptune, 2008), walking (e.g., Anderson and Pandy, 2001; Neptune et al., 2004) and running (e.g., Miller et al., 2012; Sasaki and Neptune, 2006). More recently, simulations have been applied to analyzing wheelchair propulsion to identify individual muscle contributions to push and recovery mechanics (e.g., Rankin et al., 2010, 2011, 2012). Simulations can also be used to systematically vary system parameters and analyze their influence on specific biomechanical measures. Such studies have recently been used to optimize the design of bicycle configurations (e.g., Rankin and Neptune, 2010) and lower limb prostheses (e.g., Fey et al., 2012).

The purpose of this study was to use forward dynamics simulations of wheelchair propulsion to investigate how seat position influences upper extremity demand including muscle stress, co-contraction and metabolic cost. Understanding these relationships can help guide clinicians in determining the optimal wheelchair configuration to reduce upper extremity demand, and ultimately overuse injuries and pain in wheelchair users.

2. Methods

2.1. Musculoskeletal model

The musculoskeletal model used in this study was based on a previously described upper extremity model representing a 50th percentile able-bodied male (Holzbaur et al., 2005; Rankin et al., 2010, 2011) and will be summarized here (Fig. 1). The model was developed using SIMM (Musculographics, Inc., Santa Rosa, CA, USA) and consisted of a trunk and right side upper arm, forearm and hand segments. There were three degrees-of-freedom (DoFs) at the shoulder, defined as plane of elevation, elevation angle and internal–external rotation. The motion at the shoulder also included a scapulohumeral rhythm based on regression equations derived from cadaver data (Holzbaur et al., 2005). The model had two additional DoFs, elbow flexion–extension and forearm pronation–supination. The wrist was fixed in the standard anatomical position.

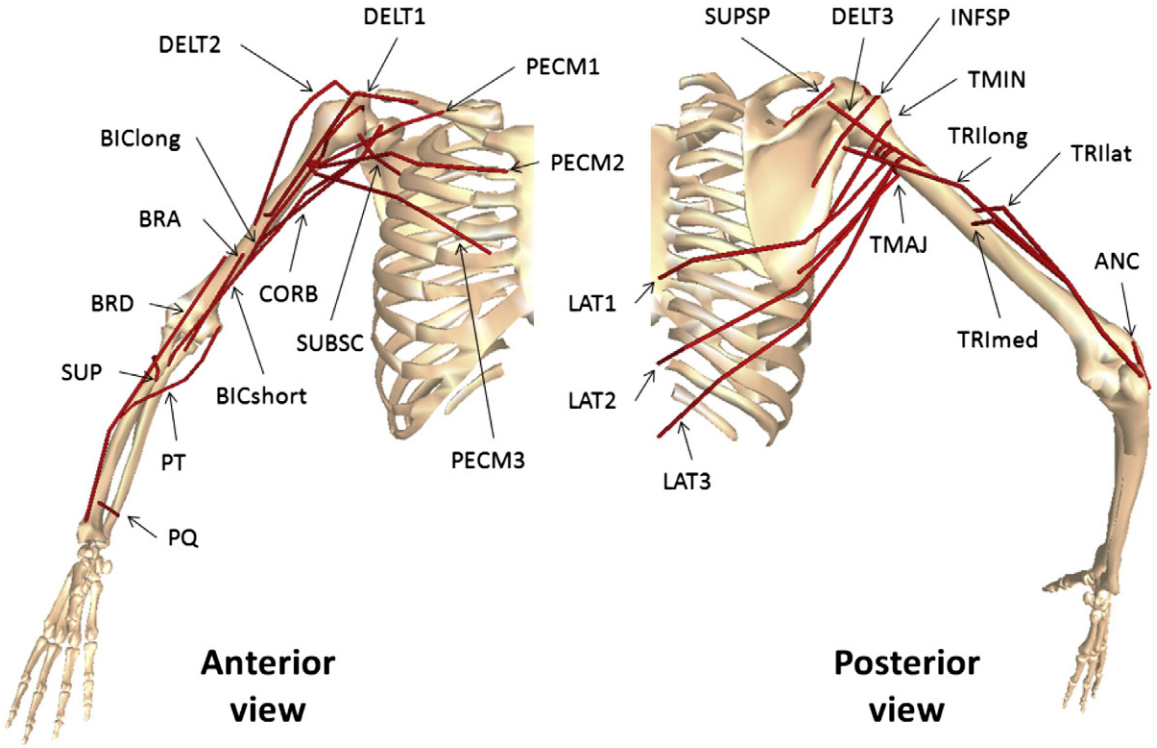

Fig. 1. 3D musculoskeletal model used in the wheelchair propulsion simulations. The model had 5 degrees-of-freedom: plane of elevation, elevation angle, internal–external rotation, elbow flexion–extension and forearm pronation–supination. Twenty-six Hill-type musculotendon actuators represented the major upper extremity muscles crossing the shoulder and elbow joints. These actuators were: DELT1 (anterior deltoid), DELT2 (middle deltoid), DELT3 (posterior deltoid), PECM1 (pectoralis major, clavicular head), PECM2 (pectoralis major, sternocostal head portion 1 — sternum), PECM3 (pectoralis major, sternocostal head portion 2 — ribs), CORB (coracobrachialis), TMAJ (teres major), LAT1 (latissimus dorsi, thoracic portion), LAT2 (latissimus dorsi, lumbar portion), LAT3 (latissimus dorsi, iliac portion), SUBSC (subscapularis), INFSP (infraspinatus), TMIN (teres minor), SUPSP (supraspinatus), BRD (brachioradialis), BRA (brachialis), BICshort (biceps brachii, short head), BIClong (biceps brachii, long head), ANC (anconeus), TRIlat (triceps brachii, lateral head), TRImed (triceps brachii, medial head), TRIlong (triceps brachii, long head), SUP (supinator), PQ (pronator quadratus) and PT (pronator teres).

Twenty-six Hill-type musculotendon actuators (Fig. 1; Table A1 in the Supplementary material) represented the major upper extremity muscles crossing the shoulder and elbow joints. Each actuator received its own excitation pattern, with the exception of three muscle groups: the two actuators that represented the sternocostal portion of the pectoralis major, the three latissimus dorsi actuators and the two actuators representing the lateral triceps and anconeus. Within each of these groups, the actuators received the same excitation pattern, resulting in a total of twenty-two independent excitation patterns. The actuators were governed by intrinsic muscle force–length–velocity relationships, and the muscle excitation–activation dynamics were modeled using a first-order differential equation (Raasch et al., 1997) with muscle-specific activation/deactivation time constants (Happee and van der Helm, 1995; Winters and Stark, 1988). Musculotendon lengths and moment arms were determined using regression equations (Rankin and Neptune, 2012). The muscle forces were applied to the model using moments applied at the appropriate joints, with the moment magnitude determined as the product of the muscle moment arm and force. Passive torques were applied at the shoulder and elbow to represent ligaments and other passive joint structures that limit extreme joint positions. The dynamic equations-of-motion were generated using SD/FAST (Parametric Technology Corp., Needham, MA, USA).

2.2. Manual wheelchair model

A model of a standard manual wheelchair with circular handrims (radius (R_{HR}) of 0.267 m, rim-to-rim distance of 0.635 m) was generated and combined with the musculoskeletal model by defining the position of the hip relative to the rear axle of the wheelchair. This position was kept fixed throughout each simulation of wheelchair propulsion and was systematically varied in both the superior/inferior and anterior/posterior directions to represent a wide range of seat positions. The motion of the third metacarpophalangeal joint was prescribed to follow a path on the circular handrim during the push phase, which was further defined by the contact (θ_C) and release (θ_R) angles. These angles were dependent on the seat position, and thus were calculated using a simple 2D model (Fig. 2; based on Richter, 2001) as follows:

$$L_{HS} = \sqrt{x_{HS}^2 + y_{HS}^2} \tag{1}$$

$$\theta_{HS} = \tan^{-1}\left(\frac{x_{HS}}{y_{HS}}\right) \tag{2}$$

$$\theta_C = 0.9 * \left(\theta_{HS} - \cos^{-1}\left[\frac{{L_{HS}}^2 + (R_{HR} + L_{FA})^2 - {L_{UA}}^2}{2L_{HS}(R_{HR} + L_{FA})}\right]\right) \tag{3}$$

$$\theta_R = 0.9 * \left(\theta_{HS} - \cos^{-1}\left[\frac{{R_{HR}}^2 + {L_{HS}}^2 - (L_{UA} + L_{FA})^2}{2R_{HR}L_{HS}}\right]\right) \tag{4}$$

where

L_{UA}	Length of the upper arm segment (0.267 m)
L_{FA}	Length of the forearm/hand segment (0.333 m)
x_{HS}	Anterior distance between the wheelchair axle/hub and shoulder
y_{HS}	Superior distance between the wheelchair axle/hub and shoulder
L_{HS}	Distance between the wheelchair axle/hub and shoulder
θ_{HS}	Angle of the vector from the wheelchair axle/hub to shoulder
θ_C	Contact angle
θ_R	Release angle

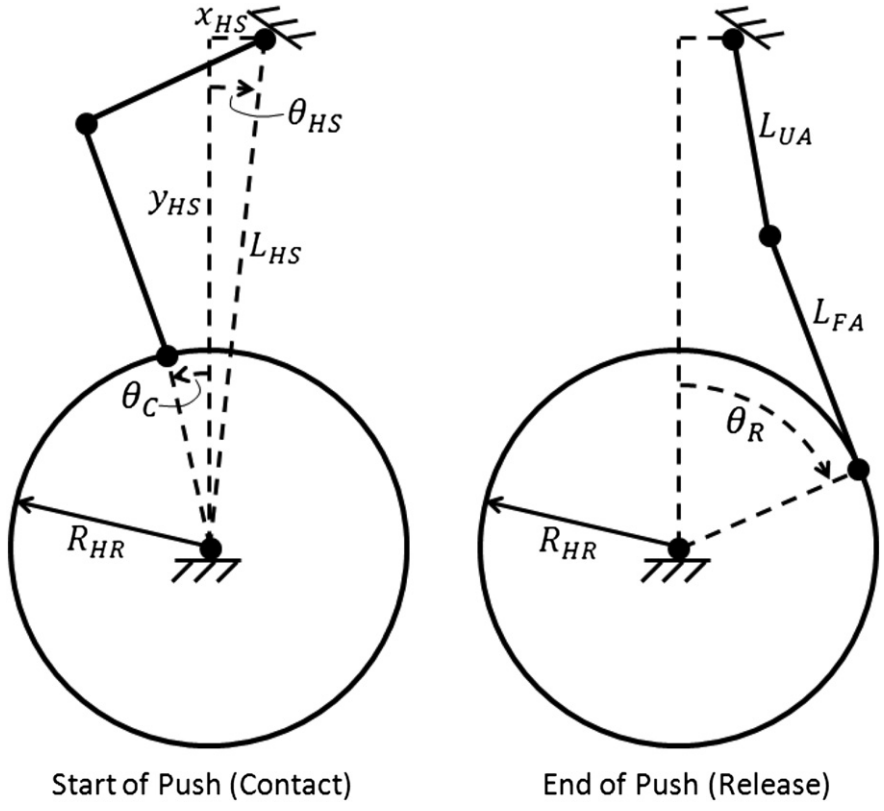

Fig. 2. Kinematic model of wheelchair propulsion used to determine contact and release angles (θ_C and θ_R, respectively). The model consisted of an upper arm (length = L_{UA}), a forearm/hand segment (length = L_{FA}) and a wheel/handrim segment (radius = R_{HR}) with revolute joints at the shoulder, elbow, hand and hub/axle. The shoulder was set at a fixed position relative to the hub/axle (total distance = L_{HS}, anterior/posterior component = x_{HS}, superior/inferior component = y_{HS}).

The push angle (θ_P) was then defined as the difference between the release angle and contact angle as:

$$\theta_p = \theta_R - \theta_C. \quad (5)$$

Additional constraints ensured that the simulations emulated realistic submaximal propulsion mechanics. For all seat positions, the average power output to the handrim was set at 10 W (Lin et al., 2009). For the initial seat position ($x_{HS} = 0.0$, $y_{HS} = 0.75$ m), the push frequency (f_P) was set at 1 Hz (PVACSCM, 2005), which yields a cycle time (t_C) of 1 s. For all other seat positions, the push frequency was determined as:

$$f_p = f_{pi}\left(\theta_{pi}/\theta_p\right) \quad (6)$$

where f_{Pi} is the push frequency and θ_{Pi} is the push angle for the initial simulation (Richter, 2001).

The push time (t_P) was set to 40% of the cycle time (Lin et al., 2009). Three propulsion cycles were simulated, and the third cycle initial and final joint angles, velocities and accelerations were compared to ensure that the simulation had reached steady-state.

The initial seat position ($x_{HS} = 0.0$, $y_{HS} = 0.75$ m) was chosen to be both near the center of the range of previously investigated seat positions (e.g., Boninger et al., 2000; Gorce and Louis, 2012; Kotajarvi et al., 2004) and near the midpoint of achievable seat positions in the model. The position was then systematically varied independently in the superior/inferior direction (0.05 m increments) and the anterior/posterior direction (0.10 m increments) throughout the range of achievable seat positions. This resulted in 53 seat positions with x_{HS} values that ranged from −0.5 m to 0.4 m and y_{HS} values that ranged from 0.35 m to 0.85 m. Note that due to concerns for wheelchair stability, not all of these seat positions can be achieved in a standard manual wheelchair. However, we included this full range of positions in our study to ascertain whether these seat positions would be favorable if stability concerns were overcome by a novel design.

2.3. Simulation of wheelchair propulsion

To simulate manual wheelchair propulsion at each seat position, we used dynamic optimization to identify the muscle excitation patterns that minimized the change in hand force and joint moments produced by the muscles (described below). The excitation pattern ($u(t)$) of each muscle group was defined as a sum of four Henning patterns (e.g., Rankin et al., 2011) as:

$$u(t) = \sum_{i=1}^{4} u_i(t) \quad (7)$$

where $u_i(t)$ is the excitation value at time t for the i^{th} Henning pattern. Each Henning pattern was defined as:

$$u_i(t) = \begin{cases} \frac{m_i}{2}\left[1-\cos\left(\frac{2\pi(t-a_i)}{b_i-a_i}\right)\right] & , \quad a_i \le t \le b_i \\ 0 & , \quad \text{otherwise} \end{cases} \quad (8)$$

where m_i, a_i and b_i are the magnitude, onset and offset, respectively. This resulted in 12 parameters for each muscle group (264 total parameters).

A simulated annealing optimization algorithm (Goffe et al., 1994) was used to find the optimal muscle excitation parameters that simulated wheelchair propulsion and minimized the change in hand force and moments (Ohta et al., 2004), with the cost function defined as:

$$J = \int_0^{t_c}\left(\dot{F}^T\dot{F} + w\dot{\tau}^T\dot{\tau}\right)dt \quad (9)$$

where $\dot{F}$ is the vector containing the time derivatives of tangential, radial and lateral components of the simulation handrim force (in units of N), $\dot{\tau}$ is the vector of the time derivatives of the simulation joint moments produced by individual muscle forces (N m), and w is a weighting factor (m^{-2}). The weighting factor was set at 50 m^{-2}.

2.4. Simulation analysis

All simulation analyses were performed on the third propulsion cycle after the simulation had reached steady-state. The seat positions were originally defined as anterior and superior offsets from the initial position ($x_{HS} = 0.0$, $y_{HS} = 0.75$ m) with negative numbers denoting posterior and inferior positions, but in order to transform these positions into a coordinate system that scales with subject anthropometry, the elbow flexion angle and angle of the hub-shoulder vector were also determined when the hand was at TDC. For the initial seat position, simulation mechanics were compared to the group-averaged experimental mechanics of 12 experienced wheelchair users (from Rankin et al., 2011). For all seat positions, individual muscle stress, level of co-contraction and metabolic cost were calculated.

Individual muscle stress (muscle force divided by the physiological cross-sectional area) was calculated at each time step. Stress values were then averaged across all of the muscles over the entire cycle to provide a measure of the overall upper extremity muscle stress (σ_{ue}):

$$\sigma_{ue} = \frac{1}{t_c}\int_0^{t_c}\left(\frac{1}{n_{mus}}\sum_{i=1}^{n_{mus}}\sigma_i(t)\right)dt \quad (10)$$

where n_{mus} is the total number of muscles in the model. The maximum possible stress level was set at 0.8 MPa (Crowninshield and Brand, 1981).

Muscle co-contraction was examined by determining the average total magnitude of joint moments produced by the muscle forces (τ_{total}) and average net moment produced by the sum of these muscle-produced moments (τ_{net}) and defining the co-contraction moment (τ_{cc}) as the difference between these measures:

$$\tau_{total} = \frac{1}{n_{DoF*}t_c}\int_0^{t_c}\left(\sum_{j=1}^{n_{DoF}}\sum_{i=1}^{n_{mus}}\left|\tau_{i,j}(t)\right)\right)dt \quad (11)$$

$$\tau_{net} = \frac{1}{n_{DoF*}t_c}\int_0^{t_c}\left(\left|\sum_{j=1}^{n_{DoF}}\sum_{j=1}^{n_{mus}}\tau_{i,j}(t)\right|\right)dt \quad (12)$$

$$\tau_{cc} = \tau_{total} - \tau_{net} \quad (13)$$

where n_{DoF} is the number of DoFs being examined and $\tau_{i,j}$ is the moment that the i^{th} muscle applies about the j^{th} degree-of-freedom. This measure is equivalent to twice the average negative moment (i.e., the moment in the direction opposite to that of the net moment), which would be the upper limit in co-contraction.

Finally, metabolic cost was calculated using a previously described model (Umberger, 2010; Umberger et al., 2003) by determining the rate of metabolic energy expenditure at each time step and integrating over the entire cycle. This value was then normalized by the total work done on the handrim throughout the cycle. The fiber type composition values used in the model (i.e. percentage of fast-twitch fibers) were based on previously published data (Johnson et al., 1973).

3. Results

The forward dynamics simulations successfully emulated normal wheelchair propulsion mechanics, with the average difference between the experimental and initial position simulation kinematics within 1.4 standard deviations (SDs) of the experimental average and handrim kinetics within 1.1 SDs (Table 1). The initial simulation contact, release and push angles were all within 1.0 SDs from the experimental averages as well. All simulations used an under-rim

Table 1
Average differences between initial position simulation mechanics and group-averaged experimental mechanics of 12 experienced wheelchair users (from Rankin et al., 2011). For comparison, two standard deviations (SDs) of the experimental data are provided to indicate inter-subject variability.

	Simulation difference	Experimental variability (2 SDs)
Shoulder plane of elevation (deg)	9.8	12.0
Shoulder elevation angle (deg)	7.7	28.8
Shoulder internal–external rotation (deg)	16.3	30.8
Elbow flexion–extension (deg)	22.9	25.0
Forearm pronation–supination (deg)	31.8	26.2
All degrees-of-freedom (deg)	17.7	24.6
Handrim tangential force (N)	14.0	15.5
Handrim radial force (N)	11.0	18.8
Handrim lateral force (N)	2.6	15.6
All forces (N)	9.2	16.7
Contact angle (deg)	9.3	33.8
Release angle (deg)	6.8	30.1
Push angle (deg)	16.1	33.8

recovery pattern (Fig. 3), which is characterized by the hand dropping below the handrim as it returns to the position of initial handrim contact (e.g., Kwarciak et al., 2012). This type of recovery pattern has been recommended in recent guidelines (e.g., Kwarciak et al., 2012; PVACSCM, 2005).

Across the range of seat positions, there were clear regions where muscle stress, co-contraction and metabolic cost were minimized.

3.1. The influence of seat position on muscle stress

The overall muscle stress (Fig. 4) was minimized (72.2 kPa, 9.0% of the maximum possible stress level) at a seat position with anterior and superior offsets of −0.16 m and 0.01 m (hub-shoulder angle: −11.5°, TDC elbow angle: 116.9°). Seat positions with anterior offsets between −0.20 m and −0.01 m (hub-shoulder angle: between −15° and 0) and superior offsets between −0.03 m and 0.03 m (TDC elbow angle: between 105° and 120°) had an associated overall muscle stress level less than 85 kPa (10.6% of the maximum possible stress level). There was a smaller secondary range of seat positions with anterior offsets between −0.20 m and −0.16 m (hub-shoulder angle: between −20° and −12.5°) and superior offsets between −0.16 m and −0.13 m (TDC elbow angle: between 80° and 85°) that also had an overall muscle stress below this level. The maximum stress (150.2 kPa, 18.8% of the maximum possible stress level) occurred at a seat position with anterior and superior offsets of −0.10 m and 0.10 m, respectively (hub-shoulder angle: −6.4°, TDC elbow angle: 149.6°).

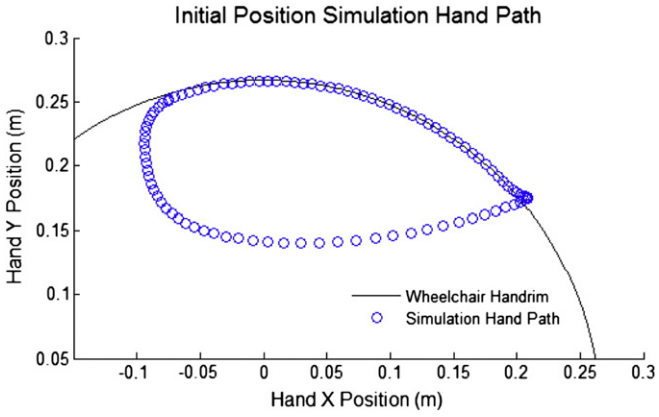

Fig. 3. Initial position simulation hand trajectory. The wheelchair handrim is represented by a solid line and the simulation hand path is represented by circles.

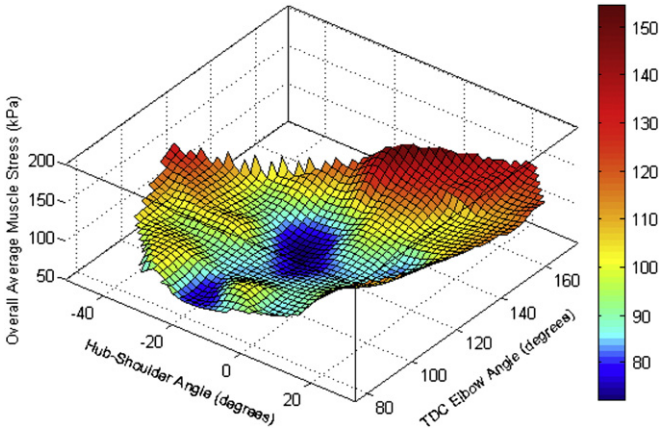

Fig. 4. Overall muscle stress versus seat position. Seat position is defined by the hub-shoulder angle and elbow angle when the hand is at top-dead-center.

3.2. The influence of seat position on muscle co-contraction

The average co-contraction moment across all DoFs (Fig. 5) was minimized (4.6 Nm) at a seat position with anterior and superior offsets of −0.09 m and 0.04 m (hub-shoulder angle: −6.4°, TDC elbow angle: 122.2°). Seat positions with anterior offsets between −0.14 m and −0.03 m (hub-shoulder angle: between −10° and −2.5°) and superior offsets between −0.01 m and 0.05 m (TDC elbow angle: between 110° and 130°) had an average co-contraction moment of less than 5 Nm. The maximum average co-contraction moment (14.0 Nm) occurred at a seat position with anterior and superior offsets of 0.30 m and −0.10 m, respectively (hub-shoulder angle: 25.1°, TDC elbow angle: 117.5°).

3.3. The influence of seat position on metabolic cost

The normalized metabolic cost (Fig. 6) was minimized (8.5) at a seat position with anterior and superior offsets from the initial position of −0.15 m and −0.03 m, respectively (hub-shoulder angle: −11.6°, TDC elbow angle: 106.6°). Seat positions with anterior offsets between −0.20 m and 0.13 m (hub-shoulder angle: between −15° and 10°) and superior offsets between −0.05 m and 0.03 m (TDC elbow angle: between 100° and 120°) had an associated normalized metabolic cost less than 10. There was a smaller secondary range of seat positions with anterior offsets between −0.20 m and −0.17 m (hub-shoulder angle: between −20° and −15°) and superior offsets between −0.16 m and 0.13 m (TDC elbow angle: between 80° and

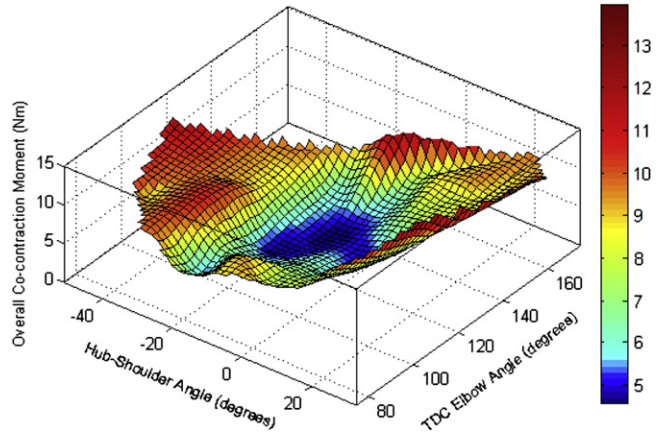

Fig. 5. Average co-contraction moment versus seat position. Co-contraction moment is the difference between total moment and net moment. Seat position is defined by the hub-shoulder angle and elbow angle when the hand is at top-dead-center.

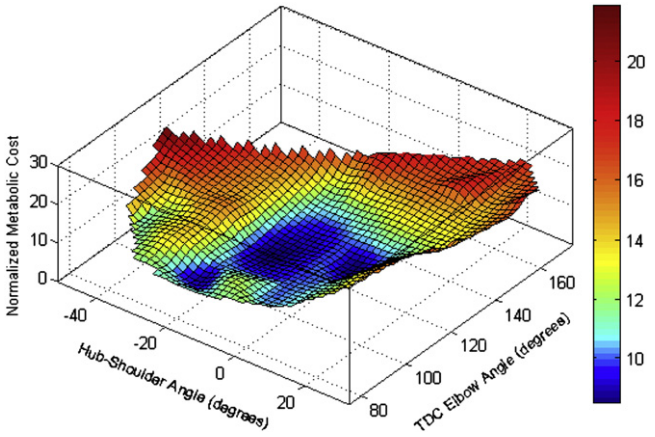

Fig. 6. Metabolic cost normalized by the total work done on the handrim versus seat position. Seat position is defined by the hub-shoulder angle and elbow angle when the hand is at top-dead-center.

85°) that also had a normalized metabolic cost below this level. The maximum metabolic cost (22.3) occurred at a seat position with anterior and superior offsets of −0.50 m and −0.35 m, respectively (hub-shoulder angle: −51.1°, TDC elbow angle: 110.0°).

4. Discussion

The purpose of this study was to identify the influence of wheelchair seat position on upper extremity demand using a musculoskeletal model and forward dynamics simulations of manual wheelchair propulsion. This approach allowed a detailed analysis of direct measures of upper extremity demand (i.e., muscle stress, co-contraction and metabolic cost) across a range of feasible seat positions. Muscle stress, co-contraction and metabolic cost were all near minimum values at seat positions with an anterior offset between −0.14 m and −0.03 m (hub-shoulder angle: between −10° and −2.5°) and a superior offset between −0.01 m and 0.03 m (TDC elbow angle: between 110° and 120°).

The optimal seat superior/inferior positions were similar to the recommendations of previous investigators (e.g., PVACSCM, 2005; Requejo et al., 2008; van der Woude et al., 2009). An early study suggested that biomechanical efficiency is maximized at superior/inferior seat positions between 100° and 120° TDC elbow angles (van der Woude et al., 1989), while a more recent study expanded that range to include 130° (van der Woude et al., 2009).

One study analyzing muscle activity recommended low superior/inferior seat positions (Masse et al., 1992) while another warned against moving the seat too low (Louis and Gorce, 2010). While it has also been cautioned that joint ranges of motion increase with lower seat positions (e.g., Gorce and Louis, 2012; Wei et al., 2003), superior/inferior seat position recommendations based on spatio-temporal variables such as cadence and push angle advocate TDC elbow angles between 100° and 120° (e.g., PVACSCM, 2005; Requejo et al., 2008).

The results of the current study suggest that upper extremity demand is minimized at superior/inferior seat positions with TDC elbow angles between 110° and 120°. Increased muscle stress, co-contraction and metabolic cost resulted from seat positions outside this range. This occurred despite the improvements in push angles and cadences that accompanied more inferior positions and the favorable reductions in joint ranges of motion that accompanied more superior positions.

Most seat position studies have only examined positions where the shoulder is either anterior or slightly posterior to the axle, which is likely due to concerns for wheelchair stability. As a result, whether the studies focused on improving muscle activity (e.g., Gutierrez et al., 2005), spatiotemporal variables (e.g., Boninger et al., 2000), kinetics (e.g., Mulroy et al., 2005), or a combination of these factors (e.g., PVACSCM, 2005; Requejo et al., 2008), they have often concluded that the seat should be set in the most posterior position that does not compromise the stability of the wheelchair. However, our results suggest that even if stability concerns could be addressed with a novel wheelchair design, there is a limit to how far posterior one should position the seat, as we found that the measures of upper extremity demand we investigated begin to increase once you move posterior beyond the −10° hub-shoulder angle. Further analysis showed that more posterior positions placed some of the major power-producing muscles of the push phase (e.g., anterior deltoid and pectoralis major) under non-optimal operating conditions (i.e. less favorable regions of the intrinsic muscle force–length relationship).

Since the model was driven by muscle moments, we could not directly determine the joint contact forces. However, since muscle co-contraction acts to compress the joint and increase the joint loading, our measure of co-contraction (quantified by the average co-contraction moment) provides some insight into the influence of seat position on joint contact forces. To identify which degrees-of-freedom were the primary contributors to the total co-contraction moment and most sensitive to changes in seat position, we performed a post-hoc analysis that decomposed the total co-contraction moment into contributions at each degree-of-freedom. Minimum co-contraction moments for the individual degrees-of-freedom were found at TDC elbow angles between 114.7° and 123.2°, while the anterior/posterior positions varied from −35° to −3.7° hub-shoulder angle (Table 2; Figs. A1–A5 in the Supplementary material). The moment associated with the elevation angle was the largest contributor to the total co-contraction moment, while the moments associated with the other two glenohumeral joint DoFs were the next largest. In addition, the moment associated with plane of elevation had the largest percent difference between its minimum and maximum values. The moments about the shoulder degrees-of-freedom are produced by the muscles crossing the glenohumeral joint, and consequently these muscles predominantly influenced the co-contraction trends. This highlights the importance of glenohumeral joint musculature during manual wheelchair propulsion and the influence of seat position on the potential for injury to these muscles.

A potential limitation of this study was that it did not consider the range of propulsion techniques utilized by wheelchair users. Spatial (i.e. contact angle, release angle) and temporal (i.e. push time, cadence) variables are influenced by propulsion technique and differences in

Table 2
Individual degree-of-freedom co-contraction moment values. Minimum values for each DoF and their associated hub-shoulder angles and TDC elbow angles are provided. Maximum values are provided for comparison.

		Plane of elevation	Elevation angle	Internal–external rotation	Elbow flexion–extension	Forearm pronation–supination	Overall (all DoFs)
Minimum co-contraction moment	Hub-shoulder angle (°)	−5.9	−6.3	−3.7	−34.3	−35.0	−6.4
	TDC elbow angle (°)	119.9	120.8	123.2	114.7	118.9	122.2
	Value (N m)	1.9	8.0	4.2	3.4	1.3	4.6
Maximum co-contraction moment value (N m)		20.8	28.2	15.6	13.3	4.8	14.0
Percent difference between minimum and maximum values		167%	112%	115%	119%	115%	101%

upper extremity impairment, training and terrain (e.g., Newsam et al., 1996; Richter et al., 2011). The wheelchair propulsion technique analyzed in this study was derived from representative spatiotemporal values (e.g., Lin et al., 2009; PVACSCM, 2005; Richter, 2001), but other techniques exist. Thus, future work should consider analyzing other techniques to assess whether similar trends exist. In addition, inter-subject variability in body anthropometrics was not considered, with the musculoskeletal model representing a 50th percentile able-bodied male. However, the physical capacity of wheelchair users varies with age, gender and nature of impairment and is generally less than that of non-wheelchair users (e.g., Haisma et al., 2006). Future work should include the development of subject-specific models to assess the general applicability of the trends found.

Another potential limitation is that the model did not include all of the trunk and wrist muscles, which could influence the metabolic cost estimates. However, the metabolic cost values corresponded to biomechanical efficiencies between 4.5% and 11.7%, which were similar to previously reported values (e.g., van der Woude et al., 2009). In addition, this study considered relative differences across seat positions, and therefore the lack of these muscles would likely not influence the study conclusions.

Finally, there is uncertainty in which criteria the neuromuscular system uses to resolve muscle redundancy during submaximal performance tasks such as wheelchair propulsion (e.g., Erdemir et al., 2007). Therefore, the cost function that minimized the change in hand force and moments used to generate the simulations may not be the one used by the nervous system during wheelchair propulsion. However, similar dynamic cost functions (minimizing change in moment and/or hand force) have frequently been used to successfully reproduce both geometrically constrained and unconstrained upper extremity movements (e.g., Ohta et al., 2004; Uno et al., 1989). In addition, the cost function produced a smooth, stable motion while limiting co-contraction similarly to functions that are based on reduction of muscle activations, forces or stresses. Thus, the cost function used in this study was deemed appropriate for generating the essential characteristics of manual wheelchair propulsion to achieve the study goals.

5. Conclusions

This study examined the influence of wheelchair seat position on upper extremity demand and found that muscle stress, co-contraction and metabolic cost were all near minimum values at positions with an anterior offset between −0.14 m and −0.03 m (hub-shoulder angle: between −10° and −2.5°) and a superior offset between −0.01 m and 0.03 m (TDC elbow angle: between 110° and 120°). Previous guidelines have recommended a seat positioned as posterior as possible without compromising the stability of the wheelchair. However, we found that even if stability concerns could be overcome, there is a limit to how far posterior one should position the seat as the measures of upper extremity demand we investigated increased once you move posterior beyond the −10° hub-shoulder angle. We also found that co-contraction of muscles crossing the glenohumeral joint was most sensitive to changes in seat position. These modeling and simulation results agree with previous clinical guidelines for positioning the seat to reduce upper extremity overuse injuries and pain for wheelchair users.

Acknowledgments

The authors thank Dr. Mark Richter for providing the experimental data used in this study and Dr. Jeff Rankin for his help with the initial model development.

Appendix A. Supplementary data

Supplementary data to this article can be found online at http://dx.doi.org/10.1016/j.clinbiomech.2013.03.004.

References

Anderson, F.C., Pandy, M.G., 2001. Dynamic optimization of human walking. J. Biomech. Eng. 123 (5), 381–390.
Boninger, M.L., Baldwin, M., Cooper, R.A., Koontz, A., Chan, L., 2000. Manual wheelchair pushrim biomechanics and axle position. Arch. Phys. Med. Rehabil. 81 (5), 608–613.
Centers for Disease Control and Prevention, 2009. Prevalence and most common causes of disability among adults — United States, 2005. MMWR Morb. Mortal. Wkly Rep. 58 (16), 421–426.
Crowninshield, R.D., Brand, R.A., 1981. A physiologically based criterion of muscle force prediction in locomotion. J. Biomech. 14 (11), 793–801.
Curtis, K.A., Drysdale, G.A., Lanza, R.D., Kolber, M., Vitolo, R.S., West, R., 1999. Shoulder pain in wheelchair users with tetraplegia and paraplegia. Arch. Phys. Med. Rehabil. 80 (4), 453–457.
Erdemir, A., McLean, S., Herzog, W., van den Bogert, A.J., 2007. Model-based estimation of muscle forces exerted during movements. Clin. Biomech. 22 (2), 131–154.
Fey, N.P., Klute, G.K., Neptune, R.R., 2012. Optimization of prosthetic foot stiffness to reduce metabolic cost and intact knee loading during below-knee amputee walking: a theoretical study. J. Biomech. Eng. 134 (11), 111005 (1–10).
Goffe, W.L., Ferrier, G.D., Rogers, J., 1994. Global optimization of statistical functions with simulated annealing. J. Econom. 60, 65–99.
Gorce, P., Louis, N., 2012. Wheelchair propulsion kinematics in beginners and expert users: influence of wheelchair settings. Clin. Biomech. 27 (1), 7–15.
Gutierrez, D.D., Mulroy, S.J., Newsam, C.J., Gronley, J.K., Perry, J., 2005. Effect of fore-aft seat position on shoulder demands during wheelchair propulsion: part 2. An electromyographic analysis. J. Spinal Cord Med. 28 (3), 222–229.
Gutierrez, D.D., Thompson, L., Kemp, B., Mulroy, S.J., 2007. The relationship of shoulder pain intensity to quality of life, physical activity, and community participation in persons with paraplegia. J. Spinal Cord Med. 30 (3), 251–255.
Haisma, J.A., van der Woude, L.H., Stam, H.J., Bergen, M.P., Sluis, T.A., Bussmann, J.B., 2006. Physical capacity in wheelchair-dependent persons with a spinal cord injury: a critical review of the literature. Spinal Cord 44 (11), 642–652.
Happee, R., van der Helm, F.C., 1995. The control of shoulder muscles during goal directed movements, an inverse dynamic analysis. J. Biomech. 28 (10), 1179–1191.
Holzbaur, K.R., Murray, W.M., Delp, S.L., 2005. A model of the upper extremity for simulating musculoskeletal surgery and analyzing neuromuscular control. Ann. Biomed. Eng. 33 (6), 829–840.
Johnson, M.A., Polgar, J., Weightman, D., Appleton, D., 1973. Data on the distribution of fibre types in thirty-six human muscles. An autopsy study. J. Neurol. Sci. 18 (1), 111–129.
Kaye, H.S., Kang, T., LaPlante, M., 2000. Mobility device use in the United States. Disability Statistics Report, 14. U. S. Department of Education, National Institute on Disability and Rehabilitation Research, Washington, DC.
Kotajarvi, B.R., Sabick, M.B., An, K.N., Zhao, K.D., Kaufman, K.R., Basford, J.R., 2004. The effect of seat position on wheelchair propulsion biomechanics. J. Rehabil. Res. Dev. 41 (3B), 403–413.
Kwarciak, A.M., Turner, J.T., Guo, L., Richter, W.M., 2012. The effects of four different stroke patterns on manual wheelchair propulsion and upper limb muscle strain. Disabil. Rehabil. Assist. Technol. 7 (6), 459–463.
Lin, C.J., Lin, P.C., Su, F.C., An, K.N., 2009. Biomechanics of wheelchair propulsion. J. Mech. Med. Biol. 9 (2), 229–242.
Louis, N., Gorce, P., 2010. Surface electromyography activity of upper limb muscle during wheelchair propulsion: influence of wheelchair configuration. Clin. Biomech. 25 (9), 879–885.
Masse, L.C., Lamontagne, M., O'Riain, M.D., 1992. Biomechanical analysis of wheelchair propulsion for various seating positions. J. Rehabil. Res. Dev. 29 (3), 12–28.
Miller, R.H., Umberger, B.R., Hamill, J., Caldwell, G.E., 2012. Evaluation of the minimum energy hypothesis and other potential optimality criteria for human running. Proc. R. Soc. B Biol. Sci. 279 (1733), 1498–1505.
Mulroy, S.J., Farrokhi, S., Newsam, C.J., Perry, J., 2004. Effects of spinal cord injury level on the activity of shoulder muscles during wheelchair propulsion: an electromyographic study. Arch. Phys. Med. Rehabil. 85 (6), 925–934.
Mulroy, S.J., Newsam, C.J., Gutierrez, D.D., Requejo, P., Gronley, J.K., Haubert, L.L., et al., 2005. Effect of fore-aft seat position on shoulder demands during wheelchair propulsion: part 1. A kinetic analysis. J. Spinal Cord Med. 28 (3), 214–221.
Neptune, R.R., Zajac, F.E., Kautz, S.A., 2004. Muscle force redistributes segmental power for body progression during walking. Gait Posture 19 (2), 194–205.
Newsam, C.J., Mulroy, S.J., Gronley, J.K., Bontrager, E.L., Perry, J., 1996. Temporal-spatial characteristics of wheelchair propulsion. Effects of level of spinal cord injury, terrain, and propulsion rate. Am. J. Phys. Med. Rehabil. 75 (4), 292–299.
Ohta, K., Svinin, M.M., Luo, Z., Hosoe, S., Laboissiere, R., 2004. Optimal trajectory formation of constrained human arm reaching movements. Biol. Cybern. 91 (1), 23–36.
Paralyzed Veterans of America Consortium for Spinal Cord Medicine, 2005. Preservation of upper limb function following spinal cord injury: a clinical practice guideline for health-care professionals. J. Spinal Cord Med. 28 (5), 434–470.
Raasch, C.C., Zajac, F.E., Ma, B., Levine, W.S., 1997. Muscle coordination of maximum-speed pedaling. J. Biomech. 30 (6), 595–602.
Rankin, J.W., Neptune, R.R., 2008. A theoretical analysis of an optimal chainring shape to maximize crank power during isokinetic pedaling. J. Biomech. 41 (7), 1494–1502.
Rankin, J.W., Neptune, R.R., 2010. The influence of seat configuration on maximal average crank power during pedaling: a simulation study. J. Appl. Biomech. 26 (4), 493–500.
Rankin, J.W., Neptune, R.R., 2012. Musculotendon lengths and moment arms for a three-dimensional upper-extremity model. J. Biomech. 45 (9), 1739–1744.
Rankin, J.W., Kwarciak, A.M., Mark Richter, W., Neptune, R.R., 2010. The influence of altering push force effectiveness on upper extremity demand during wheelchair propulsion. J. Biomech. 43 (14), 2771–2779.

Rankin, J.W., Richter, W.M., Neptune, R.R., 2011. Individual muscle contributions to push and recovery subtasks during wheelchair propulsion. J. Biomech. 44 (7), 1246–1252.
Rankin, J.W., Kwarciak, A.M., Richter, W.M., Neptune, R.R., 2012. The influence of wheelchair propulsion technique on upper extremity muscle demand: a simulation study. Clin. Biomech. 27 (9), 879–886.
Requejo, P., Mulroy, S., Haubert, L.L., Newsam, C., Gronley, J., Perry, J., 2008. Evidence-based strategies to preserve shoulder function in manual wheelchair users with spinal cord injury. Top. Spinal Cord Inj. Rehabil. 13 (4), 86–119.
Richter, W.M., 2001. The effect of seat position on manual wheelchair propulsion biomechanics: a quasi-static model-based approach. Med. Eng. Phys. 23 (10), 707–712.
Richter, W.M., Kwarciak, A.M., Guo, L., Turner, J.T., 2011. Effects of single-variable biofeedback on wheelchair handrim biomechanics. Arch. Phys. Med. Rehabil. 92 (4), 572–577.
Sasaki, K., Neptune, R.R., 2006. Muscle mechanical work and elastic energy utilization during walking and running near the preferred gait transition speed. Gait Posture 23 (3), 383–390.
Umberger, B.R., 2010. Stance and swing phase costs in human walking. J. R. Soc. Interface 7 (50), 1329–1340.
Umberger, B.R., Gerritsen, K.G., Martin, P.E., 2003. A model of human muscle energy expenditure. Comput. Meth. Biomech. Biomed. Eng. 6 (2), 99–111.
Uno, Y., Kawato, M., Suzuki, R., 1989. Formation and control of optimal trajectory in human multijoint arm movement: minimum torque-change model. Biol. Cybern. 61 (2), 89–101.
van der Helm, F.C., Veeger, H.E., 1996. Quasi-static analysis of muscle forces in the shoulder mechanism during wheelchair propulsion. J. Biomech. 29 (1), 39–52.
van der Woude, L.H., Veeger, D.J., Rozendal, R.H., Sargeant, T.J., 1989. Seat height in handrim wheelchair propulsion. J. Rehabil. Res. Dev. 26 (4), 31–50.
van der Woude, L.H.V., Bouw, A., van Wegen, J., van As, H., Veeger, D., de Groot, S., 2009. Seat height: effects on submaximal hand rim wheelchair performance during spinal cord injury rehabilitation. J. Rehabil. Med. 41 (3), 143–149.
Veeger, H.E., van der Helm, F.C., 2007. Shoulder function: the perfect compromise between mobility and stability. J. Biomech. 40 (10), 2119–2129.
Veeger, H.E., Rozendaal, L.A., van der Helm, F.C., 2002. Load on the shoulder in low intensity wheelchair propulsion. Clin. Biomech. 17 (3), 211–218.
Wei, S.H., Huang, S., Jiang, C.J., Chiu, J.C., 2003. Wrist kinematic characterization of wheelchair propulsion in various seating positions: implication to wrist pain. Clin. Biomech. 18 (6), S46–S52.
Winters, J.M., Stark, L., 1988. Estimated mechanical properties of synergistic muscles involved in movements of a variety of human joints. J. Biomech. 21 (12), 1027–1041.
Zajac, F.E., Neptune, R.R., Kautz, S.A., 2002. Biomechanics and muscle coordination of human walking. Part I: introduction to concepts, power transfer, dynamics and simulations. Gait Posture 16 (3), 215–232.